Benchmarking of a micro gas turbine model integrated with post-combustion CO_2 capture

Usman Ali[a], Carolina Font-Palma[b,*], Homam Nikpey Somehsaraei[c], Mohammad Mansouri Majoumerd[d], Muhammad Akram[a], Karen N Finney[a], Thom Best[e], Nassya B Mohd Said[a], Mohsen Assadi[c], Mohamed Pourkashanian[a]

[a]*Energy 2050, Energy Engineering Group, Department of Mechanical Engineering, University of Sheffield, Faculty of Engineering, S10 2TN, UK*
[b]*Department of Chemical Engineering, Thornton Science Park, University of Chester, CH2 4NU, UK*
[c]*Faculty of Science and Technology, University of Stavanger, 4036 Stavanger, Norway*
[d]*International Research Institute of Stavanger, P.O. Box 8046, 4068 Stavanger, Norway*
[e] *Faculty of Engineering, University of Leeds, LS2 9JT, UK*

Abstract

The deployment of post-combustion CO_2 capture on large-scale gas-fired power plants is currently progressing, hence the integration of the power and capture plants requires a good understanding of operational requirements and limitations to support this effort. This article aims to assist research in this area, by studying a micro gas turbine (MGT) integrated with an amine-based post-combustion CO_2 capture unit. Both processes were simulated using two different software tools –IPSEpro and Aspen Hysys, and validated against experimental tests. The two MGT models were benchmarked at the nominal condition, and then extended to part-loads (50 and 80 kW_e), prior to their integration with the capture plant at flue gas CO_2 concentrations between 5 and 10 mol%. Further, the performance of the MGT and capture plant when gas turbine exhaust gases were recirculated was assessed. Exhaust gas recirculation increases the CO_2 concentration, and reduces the exhaust gas flowrate and specific reboiler duty. The benchmarking of the two models revealed that the IPSEpro model can be easily adapted to new MGT cycle modifications since turbine temperatures and rotational speeds respond to reaching temperature limits; whilst a detailed rate-based approach for the capture plant in Hysys resulted in closely aligned simulation results with experimental data.

Keywords: micro gas turbine; post-combustion; amine-based carbon capture; exhaust gas recirculation

*Corresponding author: c.fontpalma@chester.ac.uk, c.fontpalma@gmail.com

1. Introduction

Higher living standards and population growth demand higher energy supplies, especially in the form of electricity. For secure energy distribution to the user, power generation currently relies heavily on fossil fuels, with a relatively small share of renewable resources [1]. Despite an increasing share of renewable energy sources in power generation, competitive prices and viable resources still make fossil-based fuels, such as coal and natural gas, an economically attractive option for electricity producers. Therefore, there is a strong need for the development and deployment of low carbon emission technologies, including carbon capture and storage (CCS) to commit to the target of limiting global temperature rise of 2°C compared to pre-industrial levels [2, 3]. Post-combustion capture is one potential route to mitigate CO_2 emissions from industrial plants, including power stations. Instead of releasing the CO_2 in the exhaust gas to the atmosphere, the captured carbon can be transported and stored safely in a number of locations, including geological formations, saline aquifers, unmineable coal beds and depleted oil and gas reserves [4].

One major challenge identified in the implementation of post-combustion carbon capture is the high-energy requirement imposed by solvent regeneration, which brings down the net electrical efficiency by approximately 8-10% points [5-9]. Hence, options for the utilization of internal and external heat extraction to meet the energy demands have been considered to outweigh the resulting energy penalty [6, 7]. Evaluation of such technical limitations and constraints is needed to improve the overall thermodynamic and economic performance of the whole system.

The CO_2 content in the exhaust of natural-gas-fired gas turbines (GT) typically varies from 3.8 to 4.4 mol% [10, 11]. Due to the low CO_2 concentration, and thus partial pressure in the exhaust gas, its integration with a post-combustion carbon capture plant introduces a major efficiency penalty [12-14]. Various innovations have been proposed, with modifications to the configuration of the basic gas turbine cycle [15, 16]; these include activities aimed at efficiency enhancements, such as steam injection and humid air turbine cycles (HAT) [17-19], and those increasing the CO_2 content of the exhaust gas, such as through adaptations like exhaust gas recirculation (EGR) [20]. This study is dedicated to the latter option as one of the best novel solutions under discussion.

In an EGR cycle, part of the exhaust gas is recirculated back to the oxidizer inlet after cooling and condensing out the moisture, while the rest is emitted or alternatively sent to the carbon capture unit. The enhanced CO_2 content in the exhaust gas with a reduced flowrate is beneficial for the integration of an EGR cycle with a CO_2 capture system. However, despite these advantages, the EGR cycle poses several technical problems that restrict the maximum amount of exhaust gas that can be recycled; for example, the increase in EGR ratio results in oxygen (O_2) starvation at the combustor inlet and thus narrow flame stability limits. Ditaranto et al. [21] reported an increase in unburned hydrocarbons (UHC) and CO emissions along with flame instability, when O_2 concentration at the combustor inlet decreases to 14 mol%. Further, experiments by Elkady et al. [22] showed stable operation for a dry low NOx (oxides of nitrogen) GE's F-class turbine combustor for EGR ratios of 35%. It has been recommended that the O_2 concentration at the combustor inlet should be kept higher than 16 mol% to maintain stable combustion and safe operation, as well as minimize unburned species [21-23].

Studies on the effect of EGR on the performance of the gas turbine and post-combustion capture system have focused on the energy penalty and cost reduction of the carbon capture system on its integration [6, 7, 11, 24-31]. Most of the literature pertains towards the studies encompassing the natural-gas-fired power plants in EGR mode with post-combustion capture system.

In order to assess different GT modifications to facilitate CO_2 capture on gas-fired power plants, micro gas turbines (MGTs) have been used due to their operational flexibility and adaptability for research in academia. However, the CO_2 concentration of the MGT is even leaner than industrial-scale natural-gas-fired gas turbines. Cameretti et al. [32, 33] showed the reduction in NOx emissions for the MGT by studying the effect of EGR on its performance by varying fuel types. With EGR in place, the efficiency of the capture process for large-scale GTs could be further improved [34-37]. The effect of the EGR ratio (varying from 40 to 55%) on the system performance and degree of CO_2 enhancement, as well as the effects of ambient conditions, are also reported in the literature, explored through the use of various process modelling tools [17, 34, 38, 39].

To support the underpinning research on CO_2 capture for GT-based plants, our research teams have developed models for a 100 kW_e micro gas turbine and integrated amine capture plant using two different software tools, namely IPSEpro and Aspen Hysys. The operational baseline for both models has been previously validated against experimental work conducted on two different Turbec T100 micro gas turbine in two different locations. However, the boundary conditions used, such as the ambient temperature and humidity, limit the comparability of both models. Therefore, through this collaboration, the MGT and amine capture models previously developed have been validated again using experimental data from a common test facility. Providing a common basis, the benchmarking results from both models, i.e. micro gas turbine and the capture process, are presented in this study. Models were first validated individually, and then adapted and integrated for EGR condition. The goal of this study is to highlight features of different software tools with different capabilities for the performance analysis of GT cycles with integrated post-combustion capture. The main objective is to deliver a reliable model at a sufficient level of detail, providing guidance for our future experimental campaigns on other innovative cycles including HAT.

2. Methodology

2.1 Micro gas turbine experiments

The UK Carbon Capture and Storage Research Centre's (UKCCSRC) Pilot-Scale Advanced CO_2 Capture Technology (PACT) National Core Facilities has two natural gas-fuelled micro-turbines, both of which are Turbec T100 PH (power and heat) designs. These can be coupled with the on-site post-combustion CO_2 capture plant, explored in Section 2.2. The Series 1 gas turbine at PACT is used for these experiments and can produce up to 100 kW_e of electrical power and up to 165 kW_{th} of thermal power. The electrical efficiency is around 30%, but the use of heat recovery components (a recuperator and heat exchanger) increases the overall efficiency to ~77%. These components are outlined in Figure 1. The engine is a single shaft

design, where the compressor is driven by the radial turbine on the same shaft, with the high-speed electrical generator (up to 70,000 rpm). The single centrifugal compressor is used to compress the ambient air until a maximum pressure ratio of ~4.5:1 is achieved. The pressurized air is then pre-heated with the hot flue gases via a recuperator to increase the electrical efficiency, before entering the combustion chamber. The natural gas is fed into the combustion chamber via a fuel booster to increase the pressure, where an electrical ignitor is then used to light the gas after it is pre-mixed with the air. The lean fuel-air mix ensures emissions of CO, UHC and NOx are low. The combustion gases at the combustor exit are at a high temperature (~950°C) and an elevated pressure (~4.5 bar); these expand through the turbine, where the pressure decreases close to atmospheric and the temperature drops to around 650°C. The hot gases from the turbine pass through the recuperator, pre-heating the inlet air and further reducing the gas temperature. These then pass through the counter-current water-gas heat exchanger to generate the hot water. The flue gases exit the system through the exhaust duct, where they are safely discharged to the atmosphere. A slip stream of the exhaust gas can be taken for post-combustion capture.

Figure 1

A key variable is the power output/set-point for the turbine. For the tests herein, the minimum load was 50 kW_e and the maximum power output tested was 80 kW_e; these characterised the operation of the engine for each condition, for a range of power outputs between these minimum and maximum levels, at 5 kW_e intervals. Each test condition was allowed to fully stabilise before measurements were taken and once stable operation was achieved, the test period lasted for at least 15 min, to comply with ISO 2314 [40]. As ambient conditions can affect results, specifically temperatures, tests were repeated covering a variety of ambient conditions.

Extensive systems monitoring was utilised to assess a wide range of gas turbine parameters and flue gas species; this was achieved through a variety of systems. Firstly, a number of gas turbine operating parameters were internally monitored with the turbines' own software – WinNAP – logging the following data:

- air inlet temperature (T1, in °C)
- calculated turbine inlet temperature (TIT Calc, in °C)
- turbine outlet temperature (TOT, in °C)
- power generated by the turbine (PGen, in kW)
- power set point (PGen Dem HMI, in kW)
- engine speed (BPS Engine, in rpm and NGt, in % of maximum)
- gas pressure (PGas, in mbar)
- opening of the pilot and main fuel valves (Pilot and Main, both in %)

Secondly, as detailed in Figure 1, additional instrumentation has been integrated into the turbine system to ensure full system's monitoring and a more comprehensive characterisation of the gas turbine cycle. Data-logging for these was achieved with LabView; the thermocouples, pressure transducers and flowmeters used are detailed in Table 1.

Thirdly, the emissions analysis assessed the levels of various gas-phase emissions in the flue gases from the gas turbine; two methods were utilised, both taking samples from the flue gas duct, as indicated in Figure 1. A GasMet FTIR DX4000 analyser and associated conditioning system characterised the majority of the species in the flue gas, using Fourier transform infrared (FTIR). This determined the levels of primarily CO_2, CO and various UHC species (CH_4, C_2H_6, C_2H_4, C_3H_8, C_6H_{14} and total hydrocarbons). A number of other gaseous species were also quantified in this manner, including water vapour, N_2O, NO, NO_2, SO_2, NH_3, CHOH and total NOx as NO_2. Although the bulk composition of the flue gas was determined via FTIR, this was unable to analyse for oxygen due to the unburned content in the flue gas consuming excess O_2 during analysis, which would result in an unreliable determination for this species. Consequently, a ServoFlex Mini Multi-Purpose 5200 gas analyser was used to analyse both O_2 and CO_2. The CO_2 readings here were used to corroborate the readings of this gas from the FTIR analyser. The O_2 content of the gas sample was assessed with paramagnetic transducers, whilst infrared transducers were used for evaluating the CO_2 level.

2.2 CO_2 capture plant

The capture plant is capable of capturing 1 TPD of CO_2 based on coal combustion flue gas and standard monoethanolamine (MEA), i.e. 30 wt. %. The absorption tower for these tests is packed with a high performance random stainless steel packing called INTALOX Metal Tower Packing (IMTP25). A detailed description of the plant is given in [41], and the bottom part of Figure 2 shows a schematic diagram of the capture plant. The stripper uses pressurised water heated up by electric elements. For these tests, the temperature of the pressurized water is maintained at 120°C for solvent regeneration. Stripper pressure was maintained at 1.2 bara.

The plant is instrumented for data logging, monitoring and control purposes. Temperatures are measured throughout the tests along the height of the absorber at different locations (at 2m, 3.3m, 5.1m and 6.8m heights from the gas entry point) for temperature profiling. Two Servomex analysers – a Servomex 4900 for O_2 and low level CO_2, as well as a Servomex 2500 for high level CO_2 were used to analyse the flue gas composition at the following locations: inlet of the absorber, exit of the absorber, exit of the wash column and CO_2 concentration at the exit of the stripper. The Servomex 4900 analyses at the absorber inlet, absorber outlet and wash column outlet, alternately. The switchover happens every 5 min and is controlled by a Programmable Logic Controller (PLC) through solenoid valves. In order to avoid condensation problems, the temperature of the heated sampling lines was maintained at 150°C. The sampling points were equipped with coalescence filters to remove droplets of water carried over by the gas. Samples of lean and rich solvent were collected at the end of each test and before changing conditions for the subsequent test. The solvent concentrations and loadings of CO_2 in the rich and lean solvent were measured for each test using titration methods, reported previously in [41].

For these tests, a slipstream, around 12% of the total gas turbine exhaust gas flow, was diverted towards the capture plant. The CO_2 concentration in the gas turbine exhaust gas was very low, so, in order to increase CO_2 concentration in the flue gas entering the capture plant, CO_2 was injected into the slipstream from a cryogenic CO_2 storage tank.

2.3 Micro gas turbine model

The Turbec T100 micro gas turbine is modelled and simulated by Aspen Hysys and IPSEpro. Using the natural gas and air compositions listed in Table 2, the steady-state models were developed. Both models are validated against the experimental data obtained through the PACT Core Facility. The layout of the process units of both MGT models is the same as the one shown in Figure 1.

Table 3 shows all the common assumptions used for modelling the MGT with both software tools at the design point.

The MGT modelling was carried out using the compressor and turbine characteristics maps. Figure 3 shows the compressor and turbine maps in terms of non-dimensional and corrected parameters such as pressure ratio, isentropic efficiency, corrected mass flowrate and corrected rotational speed. The axes' labels are not shown for confidentiality reasons.

The modelling work involved a comparison of both models using the GT baseline at ISO conditions. This was followed by part-load simulations, which were validated against experimental data. The validated model is then adapted to EGR.

2.3.1 Model 1

The Turbec T100 micro gas turbine was simulated in Aspen Hysys at the University of Sheffield. The thermodynamic property package used for property estimation is the Peng Robinson equation of state. The criterion of minimization of the total Gibbs energy is used to estimate the chemical equilibrium in the combustor. The compressor and turbine maps are implemented into the model as given in Figure 3. The model uses as input parameters fuel and air inlet conditions and TOT, along with rotational speed specifications for the compressor and turbine to interpret other variables from the characteristics maps.

2.3.2 Model 2

At the University of Stavanger, a detailed steady state thermodynamic model of the MGT T100 has been developed using a commercially available software, IPSEpro, a heat and mass balance software tool [42]. The physical properties of gas components are calculated with polynomials derived from the JANAF (i.e. Joint Army Navy Air Force) Thermodynamic Tables [42]. In IPSEpro, all calculations are performed assuming that the gas components are ideal gases. It should be noted that the model was previously validated both at design and part-load conditions against measured data obtained from an existing test facility in Stavanger, Norway [43]. However, for this study data obtained from the PACT Core facility is used for benchmarking purposes.

The model inputs are set power output and ambient conditions, i.e. air relative humidity, ambient air pressure and ambient air temperature. The TOT and TIT are constrained by the materials of construction with maximum allowable limits of 650°C and 950°C, respectively. When the limit of either TOT or TIT is reached, TIT or TOT and the rotational speed, which

is an indicator of air mass flowrate, are regulated to avoid exceeding the limit. The details of the components' equations and changes made specifically for MGT have been described in [43, 44] and thus are not further explained here.

2.4 Amine plant model

The pilot-scale amine-based CO_2 capture plant is modelled using Aspen Hysys and IPSEpro. Both models are validated against the experimental data from the PACT Core Facility. The model components include: absorber, stripper with reboiler and condenser, water wash column, cross heat exchanger, lean amine cooler and pumps for the lean and rich amine circulation around the circuit.

2.4.1 Model 1

The thermodynamic package employed for the capture plant is the Acid Gas property package of Aspen Hysys, which is based on the Electrolyte Non-Random Two Liquid thermodynamic package for liquid phase properties. However, for vapour phase properties, the Peng-Robinson thermodynamic package was used. The main equilibrium and kinetic chemical reactions are incorporated into the model; these reactions describe the chemistry between MEA and CO_2 and the formation of carbamates and bicarbamates during the absorption and stripping process. The rate-based model assumes phase and thermal equilibrium at the vapour-liquid interface and transfer resistances in the respective films, further accounting the true composition approach with rate-limiting kinetic reactions. The model in Hysys estimates the material and energy balances simultaneously based on the rate-based model with efficiency by performing calculations at each stage to determine the mass transfer flux and the Murphree efficiency of the components of interest. These calculations account for the mass transfer resistances and the rate-limiting kinetic reactions. The correlations for the mass transfer, interfacial area and pressure drop estimation are already built-in in Hysys and hence chosen. The pressure drop correlation used is based on the vendor correlation for IMTP packing. A detailed description of the model is given in [41]. As input data in the Hysys model, lean loadings were specified based on measured values.

2.4.2 Model 2

The modelling approach for the absorption/stripping processes in IPSEpro is mainly based on assuming an equilibrium state that will prevail in the bottom of the absorber and stripper. This assumption relates the partial pressure of CO_2 in the feed gas to the capture unit (or gas turbine exhaust gas) to the total amount of CO_2 that is absorbed in the solvent. This method assumes chemical, physical, and thermal equilibrium between the two phases (i.e. vapour and liquid) and does not consider the mass transfer due to chemical reactions in the interface between gas and liquid. The vapour-liquid equilibrium data that are often used to express the loading of an amine at different temperatures implemented in the IPSEpro model based on data from [45]. It is also assumed that the exhaust gas leaving the absorber is saturated with water according to Raoult's law. By these assumptions, the CO_2 concentration in the rich solvent and the maximum concentration of the acid gases remaining in the regenerated solvent could be determined. Further details are available in [46].

The models were validated against experimental data. Then, the MGT and amine plant models were integrated for full system evaluation.

3. Results and discussions

3.1 Gas turbine experimental results

Table 4 summarises the experimental data gained from the Series 1 Turbec T100 PH gas turbine tests at the PACT Core Facility, outlining the results for the gas turbine parameters and flue gas analysis over its operating envelope. As shown, there are distinct trends for a number of key parameters. The fuel and air flowrates (FR4) increased with power output, as did the engine speed. O_2 levels decreased with increasing power output, as more oxygen was consumed due to the higher fuel flowrates; a similar but opposite trend was noted for CO_2 concentrations. CO_2 peaked for the highest power output, at 1.66 vol% for 80 kW_e. As noted in Section 2.1, measurements of CO, UHC and NOx in the flue gases were indeed low for all cases, due to the high dilution. This was also the reason for the low levels of CO_2, which can impede post-combustion capture. The TOT was 645°C in all cases, whereas the TIT increased from ~880°C at baseload to ~950°C at maximum power output. Engine speeds also peaked at maximum power output (69,667 rpm).

3.2 MGT: Base case model

The base case model was developed at ISO conditions [47] for the power output of 100 kW_e. The models performance is evaluated at the design point, with the TOT of 650°C. However, for validation against experimental data, TOT was kept constant at the measured value of 645°C.

For the Hysys model, the TIT Calc resulted in 948°C when the TOT is maintained at 645ºC. The MGT is controlled in such a way that the rotational speed varies by varying the natural gas flowrate to manage the input constant TOT of 645°C. The rotational speed for the 100 kW_e was fixed as 70,000 rpm through input.

For the IPSEpro model, the TOT is kept constant at reference value which is 650 ºC. The fuel flowrate and rotational speed (air mass flow) are adjusted to generate demanded 100 kW_e power output. The calculated TIT and rotational speed are 946ºC and 69,727 rpm, respectively, which are very close to reference values given in Section 3.1 and in [48].

Table 5 shows the base case MGT calculation results for both models, which are in good agreement with the manufacturer reference data [48]. The small discrepancy in the electrical efficiency and fuel consumption is mainly due to power consumption of the auxiliaries such as buffer air pump and lubrication oil pump, which were not considered in the model. In addition, there might be a difference between the natural gas composition in this study and that used by the manufacturer. It is noteworthy that the difference in LHV values calculated by two models is mainly due to different property packages and reference values used by two software tools.

3.3 *MGT: Part-load case model*

After validation of the base case models against the manufacturer data at nominal load, simulations are extended for part-load conditions. The models are validated at different part-loads against the experimental results summarised in Table 4. Mean experimental values were used to tune the model with the power varied from 50 to 80 kW_e, with 5 kW_e intervals. Figures 3 to 5 show results of the predicted versus experimental values for selected parameters. These parameters include compressor outlet temperature and pressure (Figure 4), turbine inlet temperature (Figure 5), and rotational speed (Figure 6) for experimental, IPSEpro and Hysys reported values.

The mean percent absolute error with respect to experimental data for the compressor outlet pressure, compressor outlet temperature, turbine inlet temperature, and rotational speed for Hysys reported values are 1.97, 1.02, 3.54, and 0.46 %, respectively. As the combustor calculation is based on the minimization of Gibbs free energy rather than kinetics, this results in higher deviations of the turbine inlet temperature. Also, it must be kept in mind that the rotational speed is a fixed parameter for the model developed in Hysys.

For the IPSEpro model, the mean absolute error for the compressor outlet pressure, compressor outlet temperature, turbine inlet temperature, and rotational speed are 4.12, 0.57, 1.77 and 0.27%, respectively. Compared to the Hysys model, IPSEpro shows higher error for compressor outlet pressure calculation. However, as can be seen from Figure 4, the deviation between calculated and measured values is not significant. A maximum deviation of around 0.1 bar occurs for all operational conditions. On the other hand, the IPSEpro model shows better performance in temperatures calculations, both for compressor outlet temperature and TIT.

Both models are in good agreement with the measured values, as shown in Figures 4 to 6. This indicates that the developed models are robust enough for the application of exhaust gas recirculation to the base micro gas turbine.

3.4 Amine capture plant: Experimental results

Experimentally, around 12% of the gas turbine exhaust gas is diverted to the capture plant and CO_2 is injected into the slip stream to study the behavior of the exhaust gas recirculation on the pilot-scale amine-based CO_2 capture plant. The CO_2 concentration in the flue gas entering the absorber of the capture plant varies from 5.5 mol% to 9.9 mol%, indicating a wider workable range for the commercial-scale system. Removal rate of CO_2 was maintained at 90% for all the tests. Table 6 shows the data from the capture plant used for model verification.

3.5 Amine capture plant: modelling

The pilot-scale amine-based CO_2 capture plant models in IPSEpro and Hysys are validated against the set of experimental data presented in Table 6. The models are tuned with the measured data. The pressure drop across the height of the packing is maintained to not exceed

2.04 mbar and the approach to the maximum capacity is limited to 80% of the flooding velocity, for both absorber and stripper [49, 50]. The model results for some selected parameters are shown in Figures 7 to 9 for IPSEpro, Hysys and experimental values, along with deviations from measured values. The selected parameters include the lean and rich amine loadings, specific reboiler duty and degree of regeneration. The mean percent absolute deviation for the lean amine loading, rich amine loading, specific reboiler duty and degree of regeneration for Hysys reported values are 0.21, 2.26, 2.03 and 1.94 %, respectively while these values are 54.0, 21.1, 13.2 and 21.1 % respectively for IPSEpro model. The results show that Hysys predicted values are in good agreement with the measured values as shown in Figures 7 to 9, giving confidence that the model is reliable for integration with the MGT and further analysis. It is also shown that the predicted values by the IPSEpro model have higher uncertainties. This is mainly due to the approach used in the IPSEpro model, i.e. equilibrium stage method with its limitations (refer to Section 2.4.2) compared to a rate-based approach used in Hysys that is based on analyzing the mass and heat transfer along with chemical reactions between phases (gas and liquid). Nevertheless, different simplifications in the IPSEpro model could have minor effects in the context of the overall plant's performance evaluation, as the predicted value for the specific reboiler duty is still in good agreement with the experimental data. Moreover, skipping a large number of simultaneous equations and more complex convergence issues might be another advantage of IPSEpro model.

3.6 Integrated system

The validated MGT and CO_2 capture models were integrated and extended to study the behavior of exhaust gas recirculation on the performance of the MGT and pilot-scale capture plant. A schematic diagram of the integrated system, the MGT with EGR coupled to the CO_2 capture plant, that has been modeled using Hysys and IPSEpro is shown in Figure 10. A full description of the MGT with EGR can be found in [51, 52]; main features are described again herein. In the two models, part of the exhaust gas is circulated back to the compressor inlet of the MGT to mix with air, defined as the EGR ratio. The rest is either sent to the chimney or forwarded to the capture plant. The recycled gas is cooled and dried through a condenser in the recycle loop. There is also a booster fan in the recycle loop to deliver the recycled gas from the condenser outlet to the inlet of the compressor.

The part-load power output of 80 kW_e is chosen, being the highest power output observed during experimentation; for the performance analysis of the MGT with EGR and integrated capture plant. The model results for 80 kW_e with and without EGR are shown in Table 7, for both IPSEpro and Hysys. The EGR applied is 55% as the O_2 concentration at the combustor inlet is around 17.6 mol %, which is still higher than the limiting O_2 concentration for efficient combustion [21, 22]. The O_2 concentration at the combustor inlet is chosen following recommendations in the literature [35] for the selection of EGR ratio. The relative drop in efficiency of the MGT with EGR due to higher fuel consumption compared to the MGT without EGR is about 1.8% and 3.0% in the Hysys and IPSEpro models, respectively. The reason is as follows: by partially replacing the intake air with exhaust gas, the heat capacity of the combustion oxidant increases. Consequently, for the same amount of fuel, the temperature rise

in the combustion chamber is decreased. This causes the power output to decrease. To keep the power output constant, the heat input is increased by increasing the fuel consumption. It should be noted that the efficiency change is relatively small. In addition, the electrical power output given in Table 7 also incorporates the power consumption by the booster fan in the recycle loop. Similarly, the variation of the fuel consumption by the application of EGR accounts the effect of the EGR on the performance of the MGT. However, the exhaust gas flowrate directed towards the pilot-scale amine-based CO_2 capture plant is reduced by the same percentage as that of the EGR ratio. However, for the present study a slipstream from the exhaust gas of the MGT with EGR is directed towards the capture plant. The flowrate of the flue gas to the absorber inlet (based on the CO_2 capture capacity of 1 TPD) is kept constant for both with and without EGR cases. Further, the CO_2 content in the exhaust gas of the MGT with EGR is 2.2 times higher than that of the MGT without EGR. This results in approximately 40% reduction in the specific reboiler duty for the CO_2 capture system in both models.

To show the effects of EGR in the MGT, the specific CO_2 emissions from the MGT with and without EGR before the integration of the CO_2 capture plant to the system are reported in Table 7. The reported specific CO_2 emissions correspond to the exhaust gas after the first splitter (S1 in Figure 10) without accounting for CO_2 coming from inlet air. It is worth noting that this research paper analyses a pilot-scale system that only treats a slipstream of the exhaust gas from the MGT both with and without EGR due to capacity limitations of the CO_2 capture plant. Therefore, the specific CO_2 emissions of the overall integrated system considering a capture unit that is capable of treating a full flue gas (the flue gas stream after S1 in Figure 10) is not addressed in this study. The EGR results in about 0.2-0.3 % increase in specific CO_2 emissions, as reported in Table 7.

The performance results for CO_2 capture plant are also tabulated in Table 7, for both IPSEpro and Hysys simulation tools. The solvent concentration is fixed at 30 wt. % of MEA and the CO_2 capture rate is maintained at 90% (i.e. 90% of the CO_2 that is otherwise vented to the atmosphere is captured from the flue gas entering the absorber). The absorber inlet temperature is fixed at 40°C. As the CO_2 concentration increases, the mass transfer increases; this can be observed with the increase of the rich amine loading. Since the packing dimensions remain the same, the increased CO_2 loading in the rich amine is due to the higher driving force for the increased CO_2 concentration. The benefits of using an EGR of 55% are that the increased CO_2 concentration promotes an approximately 70% increase in the acid gas pick-up due to a higher difference between rich and amine loadings, and the specific reboiler duty decreases.

Despite the MGT resulting in slightly higher specific CO_2 emissions to the atmosphere when EGR is applied, the integration of the CO_2 capture plant results in savings in terms of the solvent regeneration energy requirements; for the flue gas with higher CO_2 concentration due to EGR application.

Application of EGR also results in more power consumption due to the booster fan in the recycle loop and an increased cooling water requirement for cooling and drying of the recycled gas. However, these drawbacks due to EGR can be offset by smaller absorber size, smaller gas/gas heat exchangers and lower regeneration energy requirements in the CO_2 capture plant.

It is reported in the literature [14] that EGR application results in about 30 % reduction in the capital cost of the CO_2 capture plant due to smaller absorption/stripping columns and reboiler. The levelised cost of electricity is decreased by 11 % [11] and 2.8 % [25] for the natural gas combined cycle power plant in EGR mode integrated with post-combustion carbon capture system, in comparison to the system without EGR. The overnight cost of the integrated plant with EGR is 43 % higher than the plant without capture, while for the integrated plant without EGR it is 45 % higher compared to the plant without capture [24].

4. Conclusions

Carbon capture on natural gas-fired power plants is in the process of being commercially demonstrated. In order to support research on this area and aid its deployment, a micro gas turbine has been selected to carry out experimental and theoretical studies, integrated with an amine-based post combustion CO_2 capture unit, due to its operational flexibility and affordability. MGT and amine capture models were developed using two different software tools, IPSEpro and Aspen Hysys. The baseline cases for both the turbine and capture plant were validated with experimental data from the PACT Core Facilities in the UK. This work shows the benchmarking of both models using a common basis, that is, the same boundary conditions and assumptions for fair comparisons (where only a slip stream of the exhaust gas from MGT is analysed for both with and without EGR), and then develops models including EGR into the turbine system to assess the impacts on post-combustion capture. EGR on gas turbines aims to increase the concentration and partial pressure of the CO_2 in the flue gases, which will subsequently decrease the energy penalty of CO_2 capture.

Given the fact that the exhaust gas of the MGT contains a low CO_2 concentration (and thus also partial pressure), exhaust gas recirculation was also studied by using validated models for each unit, i.e. the MGT and the capture plant, and then integrating them using the two aforementioned software tools. An EGR ratio of 55% was chosen to maintain an O_2 concentration at the combustor inlet of 17.6 mol% and therefore limit flame instabilities and the formation of unburned species. Both integrated EGR models produced an exhaust gas with 2.2 times the CO_2 concentration of the MGT without EGR. This increased CO_2 concentration promotes an approximately 70% increase in the acid gas pick-up and an approximately 40% decrease in the specific reboiler duty.

The benchmarking of the two models aims to provide guidance for future experimental campaigns on other innovative cycles. This work identified strengths in the models and found that both models complement each other. The IPSEpro model can be easily adapted to new MGT cycle modifications since turbine temperatures and rotational speeds respond to reaching limits of TOT or TIT. On the other hand, Hysys comprises a detailed rate-based model for the capture plant that produces results with very good agreement to experimental conditions. Future work will include experiments for CO_2 injection at the compressor inlet to study its effects on the micro-turbine.

Nomenclature

CCS	carbon capture and storage
DLN	dry low NOx
EGR	exhaust gas recirculation
FR	flowrate
FTIR	Fourier transform infrared
GE	General Electric
GT	gas turbine
HAT	humid air turbine
HEX	heat exchanger
IMTP	INTALOX Metal Tower Packing
JANAF	Joint Army Navy Air Force
LHV	lower heating value
MEA	monoethanolamine
MGT	micro gas turbine
NG	natural gas
NOx	oxides of nitrogen (NO and NO_2)
PACT	Pilot-scale Advanced Carbon-capture Technology
PGen	power generated
PH	power and heat
PLC	programmable logic controller
PT	pressure transducer
TC	thermocouple
TIT	turbine inlet temperature
TOT	turbine outlet temperature
TPD	tonnes per day
UHC	unburned hydrocarbon

UKCCSRC	The UK Carbon Capture and Storage Research Centre
PHW	Pressurised Hot Water
T_{Rin}	Temperature of pressurised hot water entering the reboiler
T_{Rout}	Temperature of pressurised hot water leaving the reboiler
T_{AC}	rich-lean cross exchanger approach temperature, cold end
T_{AH}	rich-lean cross exchanger approach temperature, hot end

Acknowledgements

The authors would like to thank for their financial support of this project: EPSRC Gas-FACTS: Gas – Future Advanced Capture Technology Options, EP/J020788/1.

U. Ali acknowledges the grant provided by the University of Engineering and Technology, Lahore Pakistan and the partial support by the University of Sheffield, UK for this research. M. Mansouri Majoumerd acknowledges the financial support provided by the International Research Institute of Stavanger (IRIS), Norway. C. Font Palma would like to acknowledge the financial support of the UK CCS Research Centre (www.ukccsrc.ac.uk) in carrying out this work. The UKCCSRC is funded by the EPSRC as part of the RCUK Energy Programme.

References

[1] DECC. Updated energy and emissions projections 2015. London, UK: Department of Energy & Climate Change; 2015.
[2] IEAGHG. UK FEED Studies 2011 - A summary. International Energy Agengy (IEA); 2013.
[3] IEAGHG. Integrated CCS project at SaskPower's Boundary Dam Power Stations. International Energy Agency (IEA); 2015.
[4] IEAGHG. Information sheets for CCS. International Energy Agency (IEA); 2013.
[5] Moller BF, Assadi M, Potts I. CO2-free power generation in combined cycles - Integration of post-combustion separation of carbon dioxide in the steam cycle. Energy. 2006;31(10-11):1520-32.
[6] Sipocz N, Assadi M. Combined Cycles With CO2 Capture: Two Alternatives for System Integration. J Eng Gas Turb Power. 2010;132(6):061701.
[7] Sipocz N, Jonshagen K, Assadi M, Genrup M. Novel High-Performing Single-Pressure Combined Cycle With CO2 Capture. J Eng Gas Turb Power. 2011;133(4):041701.
[8] Jonshagen K, Sipocz N, Genrup M. Optimal Combined Cycle for CO2 capture with EGR. Conference Optimal Combined Cycle for CO2 capture with EGR.
[9] Moller BF, Genrup M, Assadi M. On the off-design of a natural gas-fired combined cycle with CO2 capture. Energy. 2007;32(4):353-9.
[10] Canepa R, Wang M, Biliyok C, Satta A. Thermodynamic analysis of combined cycle gas turbine power plant with post-combustion CO_2 capture and exhaust gas recirculation. Proceedings of the Institution of Mechanical Engineers, Part E: Journal of Process Mechanical Engineering. 2013;227(2):89-105.

[11] Sipöcz N, Tobiesen FA. Natural gas combined cycle power plants with CO_2 capture – Opportunities to reduce cost. International Journal of Greenhouse Gas Control. 2012;7(0):98-106.
[12] Hetland J, Kvamsdal HM, Haugen G, Major F, Kårstad V, Tjellander G. Integrating a full carbon capture scheme onto a 450MWe NGCC electric power generation hub for offshore operations: Presenting the Sevan GTW concept. Applied Energy. 2009;86(11):2298-307.
[13] Lindqvist K, Jordal K, Haugen G, Hoff KA, Anantharaman R. Integration aspects of reactive absorption for post-combustion CO2 capture from NGCC (natural gas combined cycle) power plants. Energy. 2014;78:758-67.
[14] Peeters A, Faaij A, Turkenburg W. Techno-economic analysis of natural gas combined cycles with post-combustion CO2 absorption, including a detailed evaluation of the development potential. International Journal of Greenhouse gas control. 2007;1(4):396-417.
[15] Heppenstall T. Advanced gas turbine cycles for power generation: a critical review. Applied Thermal Engineering. 1998;18(9):837-46.
[16] Poullikkas A. An overview of current and future sustainable gas turbine technologies. Renewable and Sustainable Energy Reviews. 2005;9(5):409-43.
[17] Nikpey H, Majoumerd MM, Assadi M, Breuhaus P. Thermodynamic Analysis of Innovative Micro Gas Turbine Cycles. Conference Thermodynamic Analysis of Innovative Micro Gas Turbine Cycles.
[18] Majoumerd MM, Somehsaraei HN, Assadi M, Breuhaus P. Micro gas turbine configurations with carbon capture - Performance assessment using a validated thermodynamic model. Appl Therm Eng. 2014;73(1):172-84.
[19] Ali U, Best T, Finney KN, Palma CF, Hughes KJ, Ingham DB, et al. Process Simulation and Thermodynamic Analysis of a Micro Turbine with Post-combustion CO2 Capture and Exhaust Gas Recirculation. Energy Procedia. 2014;63:986-96.
[20] Earnest ER. Turbine engine with exhaust gas recirculation. Google Patents; 1981.
[21] Ditaranto M, Hals J, Bjørge T. Investigation on the in-flame NO reburning in turbine exhaust gas. Proceedings of the Combustion Institute. 2009;32(2):2659-66.
[22] ElKady AM, Ursin TP, Lynghjem A, Evulet A, Brand A. Application of exhaust gas recirculation in a DLN F-class combustion system for postcombustion carbon capture. Journal of Engineering for Gas Turbines and Power. 2009;131(3):034505.
[23] Bolland O, Mathieu P. Comparison of two CO_2 removal options in combined cycle power plants. Energy Conversion and Management. 1998;39(16):1653-63.
[24] Biliyok C, Canepa R, Wang M, Yeung H. Techno-Economic Analysis of a Natural Gas Combined Cycle Power Plant with CO_2 Capture. In: Andrzej K, Ilkka T, editors. Computer Aided Chemical Engineering: Elsevier; 2013. p. 187-92.
[25] Biliyok C, Yeung H. Evaluation of natural gas combined cycle power plant for post-combustion CO_2 capture integration. International Journal of Greenhouse Gas Control. 2013;19(0):396-405.
[26] Canepa R, Wang M. Techno-economic analysis of a CO_2 capture plant integrated with a commercial scale combined cycle gas turbine (CCGT) power plant. Applied Thermal Engineering. 2014(0).
[27] Jonshagen K, Sipöcz N, Genrup M. Optimal Combined cycle for CO_2 capture with EGR. Conference Optimal Combined cycle for CO_2 capture with EGR. American Society of Mechanical Engineers, p. 867-75.
[28] Li H, Ditaranto M, Berstad D. Technologies for increasing CO_2 concentration in exhaust gas from natural gas-fired power production with post-combustion, amine-based CO_2 capture. Energy. 2011;36(2):1124-33.

[29] Belaissaoui B, Cabot G, Cabot M-S, Willson D, Favre E. CO2 capture for gas turbines: an integrated energy-efficient process combining combustion in oxygen-enriched air, flue gas recirculation, and membrane separation. Chemical Engineering Science. 2013;97:256-63.
[30] Jonshagen K, SipÃķcz N, Genrup M. A novel approach of retrofitting a combined cycle with post combustion CO2 capture. Journal of Engineering for Gas Turbines and Power. 2011;133(1):011703.
[31] Yu B, Kum S-M, Lee C-E, Lee S. Effects of exhaust gas recirculation on the thermal efficiency and combustion characteristics for premixed combustion system. Energy. 2013;49:375-83.
[32] Cameretti MC, Tuccillo R, Piazzesi R. Study of an EGR Equipped Micro Gas Turbine supplied with bio-fuels. Applied Thermal Engineering. 2013.
[33] Cameretti MC, Piazzesi R, Reale F, Tuccillo R. Combustion simulation of an exhaust gas recirculation operated micro-gas turbine. Journal of engineering for gas turbines and power. 2009;131(5).
[34] Ali U, Best T, Finney KN, Font Palma C, Hughes KJ, Ingham DB, et al. Process Simulation and Thermodynamic Analysis of a Micro Turbine with Post-combustion CO2 Capture and Exhaust Gas Recirculation. Energy Procedia. 2014;63(0):986-96.
[35] Evulet AT, ELKady AM, Branda AR, Chinn D. On the Performance and Operability of GE's Dry Low NO_x Combustors utilizing Exhaust Gas Recirculation for PostCombustion Carbon Capture. Energy Procedia. 2009;1(1):3809-16.
[36] Akram M, Khandelwal B, Blakey S, Wilson CW. Preliminary Calculations on Post-Combustion Carbon Capture from Gas Turbines with Flue Gas Recycle. Proceedings of the ASME Turbo Expo 2013 2013.
[37] Stathopoulos P, Paschereit CO. Retrofitting micro gas turbines for wet operation. A way to increase operational flexibility in distributed CHP plants. Applied Energy. 2015;154:438-46.
[38] Ali U, Font Palma C, Hughes KJ, Ingham DB, Ma L, Pourkashanian M. Thermodynamic analysis and process system comparison of the exhaust gas recirculated, steam injected and humidified micro gas turbine. Conference Thermodynamic analysis and process system comparison of the exhaust gas recirculated, steam injected and humidified micro gas turbine, Montreal, Canada. GT2015-42454, Proceedings of ASME Turbo Expo 2015.
[39] Majoumerd MM, Somehsaraei HN, Assadi M, Breuhaus P. Micro gas turbine configurations with carbon capture-Performance assessment using a validated thermodynamic model. Applied Thermal Engineering. 2014.
[40] BSi. Gas turbines. Acceptance tests. BS ISO 2314:2009: British Standard; 2010. p. 118.
[41] Akram M, Ali U, Best T, Blakey S, Finney K, Pourkashanian M. Performance evaluation of PACT Pilot-plant for CO_2 capture from gas turbines with Exhaust Gas Recycle. International Journal of Greenhouse Gas Control. 2016;47:137-50.
[42] Simtech. IPSEpro version 4.0. Simtech Simulation Technology (Simtech). Graz, Austria2003.
[43] Nikpey Somehsaraei H, Mansouri Majoumerd M, Breuhaus P, Assadi M. Performance analysis of a biogas-fueled micro gas turbine using a validated thermodynamic model. Applied Thermal Engineering. 2014;66(1–2):181-90.
[44] Lorenz M. Modeling and Off Design Simulation of the Evaporative Gas Turbine. Lund, Sweden: Lund University, 2004.
[45] Jou F-Y, Mather AE, Otto FD. The solubility of CO2 in a 30 mass percent monoethanolamine solution. The Canadian Journal of Chemical Engineering. 1995;73(1):140-7.
[46] Fredriksson Möller B. Thermoeconomic evaluation of CO2 capture with focus on gas turbine-based power plants. : Lund University, 2005.

[47] Gas turbines – Procurement – Part 2: Standard reference conditions and ratings. ISO 3977-2:. Geneva, Switzerland: International Organization for Standardization; 1997.
[48] Turbec. Technical Description: T100 Natural Gas – T100 Mircoturbine System. 2012.
[49] Kister HZ. Distillation design: McGraw-Hill New York, 1992.
[50] Strigle RF. Packed tower design and applications: random and structured packings. 2nd ed. Houston, TX: Gulf Publishing Co., 1994.
[51] Ali U, Hughes KJ, Ingham DB, Ma L, Pourkashanian M. Effect of the CO2 enhancement on the performance of a micro gas turbine with a pilot-scale CO2 capture plant. Chem Eng Res Des. 2017;117:11-23.
[52] Ali U, Font Palma C, Hughes KJ, Ingham DB, Ma L, Pourkashanian M. Impact of the operating conditions and position of exhaust gas recirculation on the performance of a micro gas turbine. In: Gernaey KV, Huusom JK, Rafiqul G, editors. Computer Aided Chemical Engineering: Elsevier 2015. p. 2417-22.

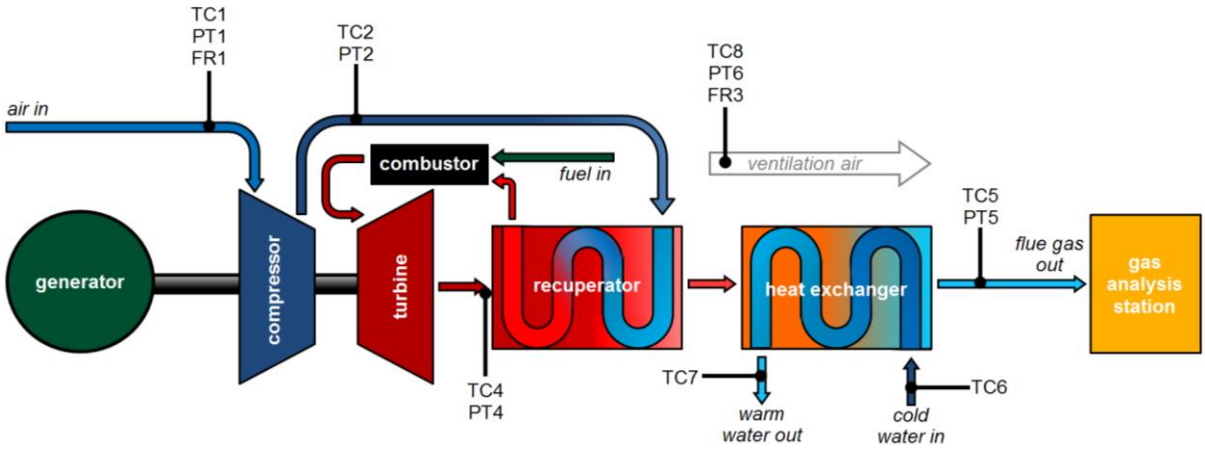

Figure 1: Key components of the Turbec T100 PH combined heat and power gas turbine system at the PACT Core facility, including the additional instrumentation (TC – thermocouples; PT – pressure transducers; FR flowrate meters).

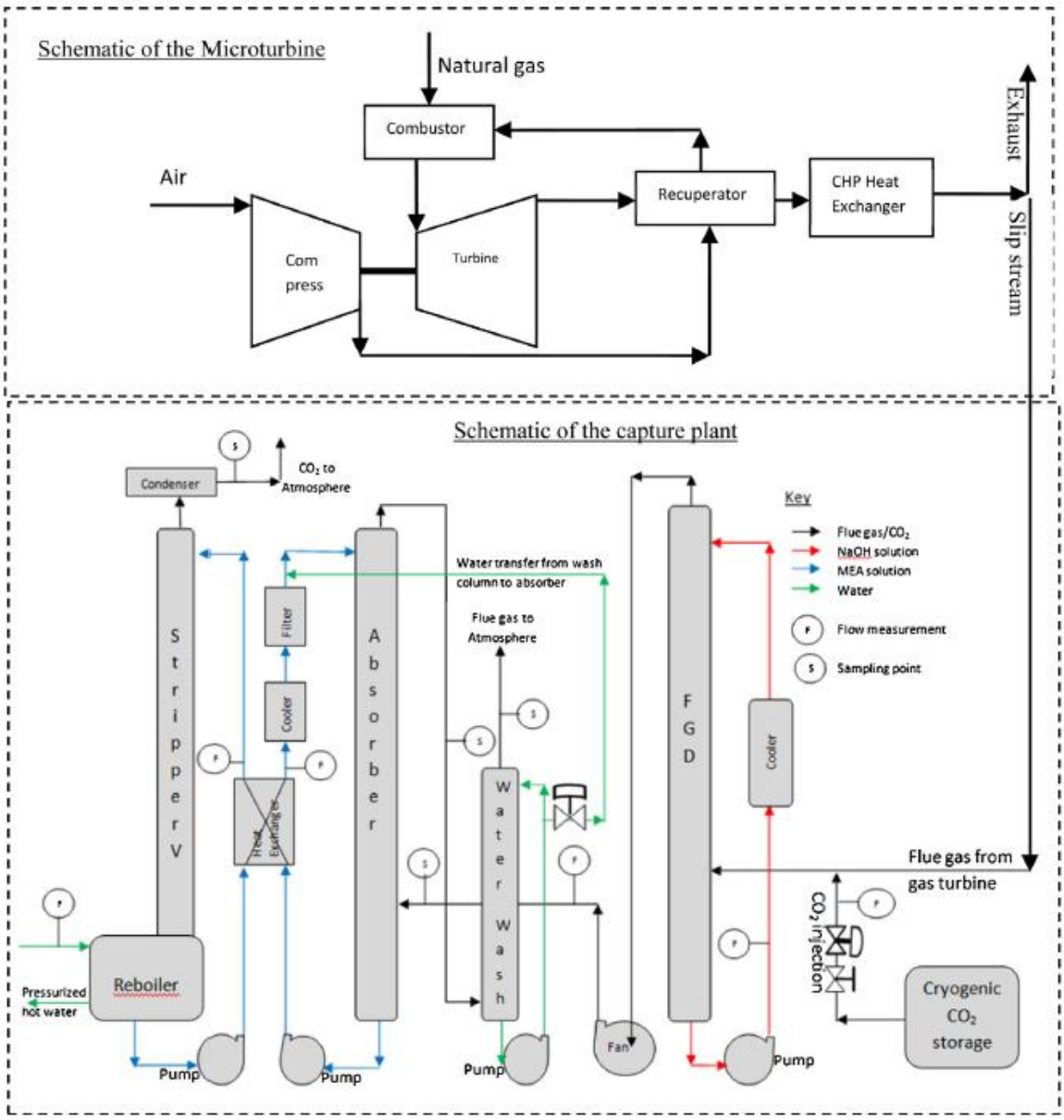

Figure 2: Schematic diagram of the experimental setup, integrated micro gas turbine and CO_2 capture plant [41]

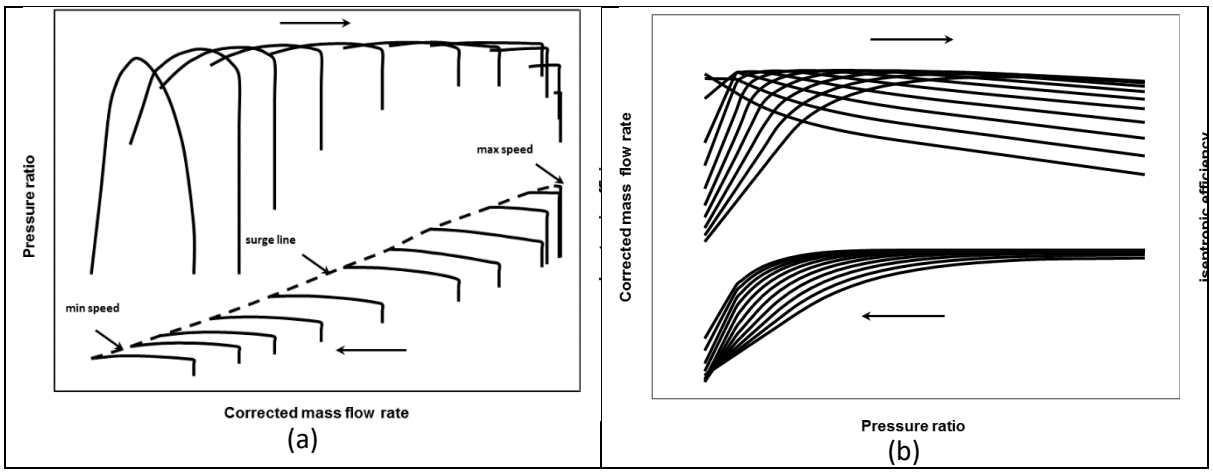

Figure 3: Compressor (a) and expander (b) characteristics maps [17]

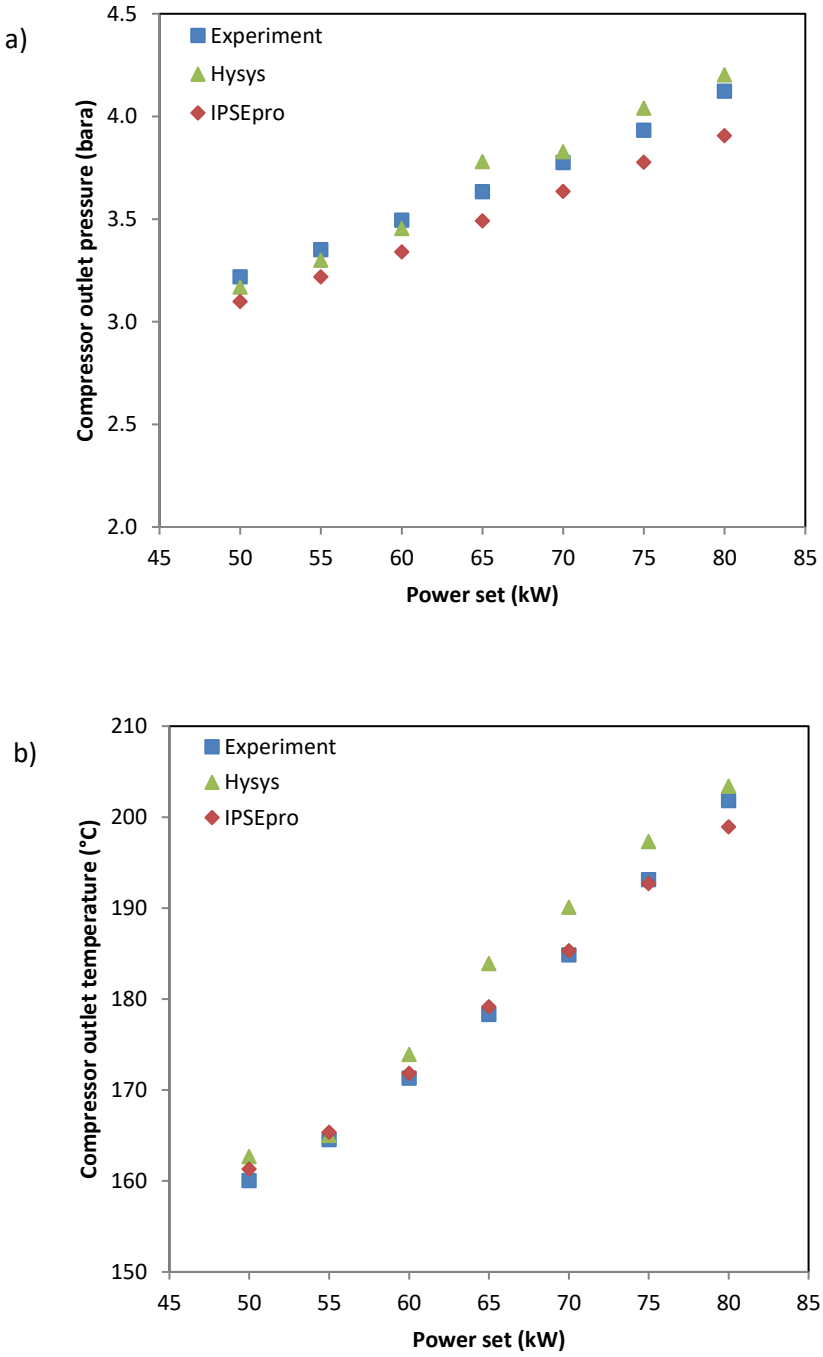

Figure 4: Compressor outlet a) pressure and b) temperature at various power outputs

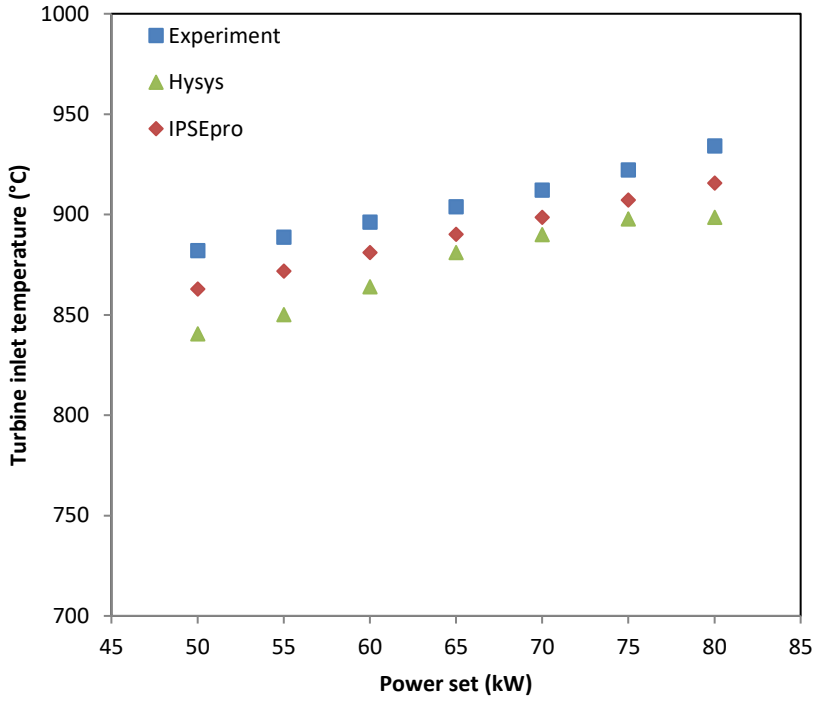

Figure 5: Turbine inlet temperature at various power outputs

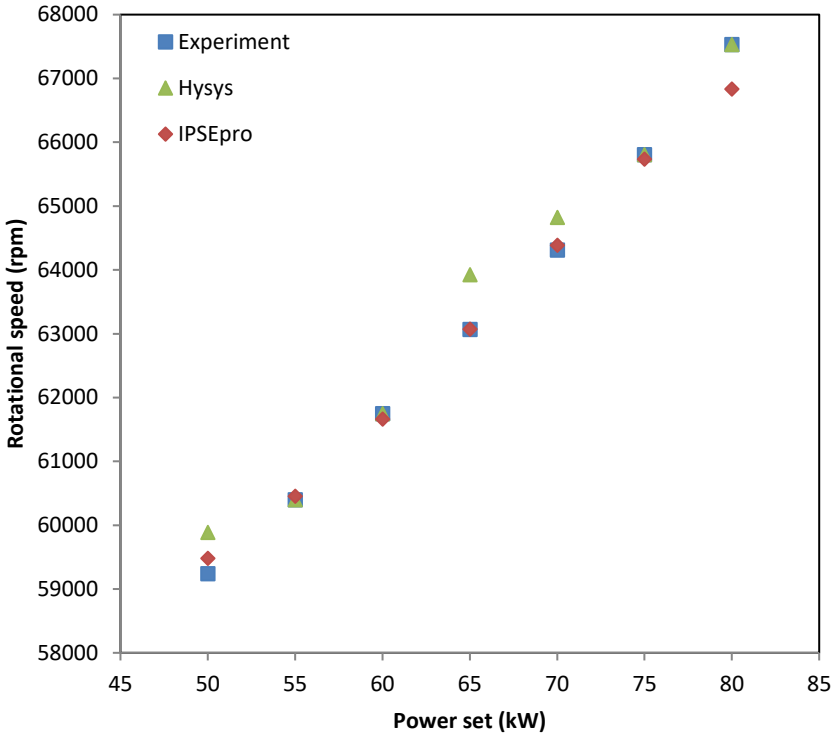

Figure 6: Rotational speed at various power outputs

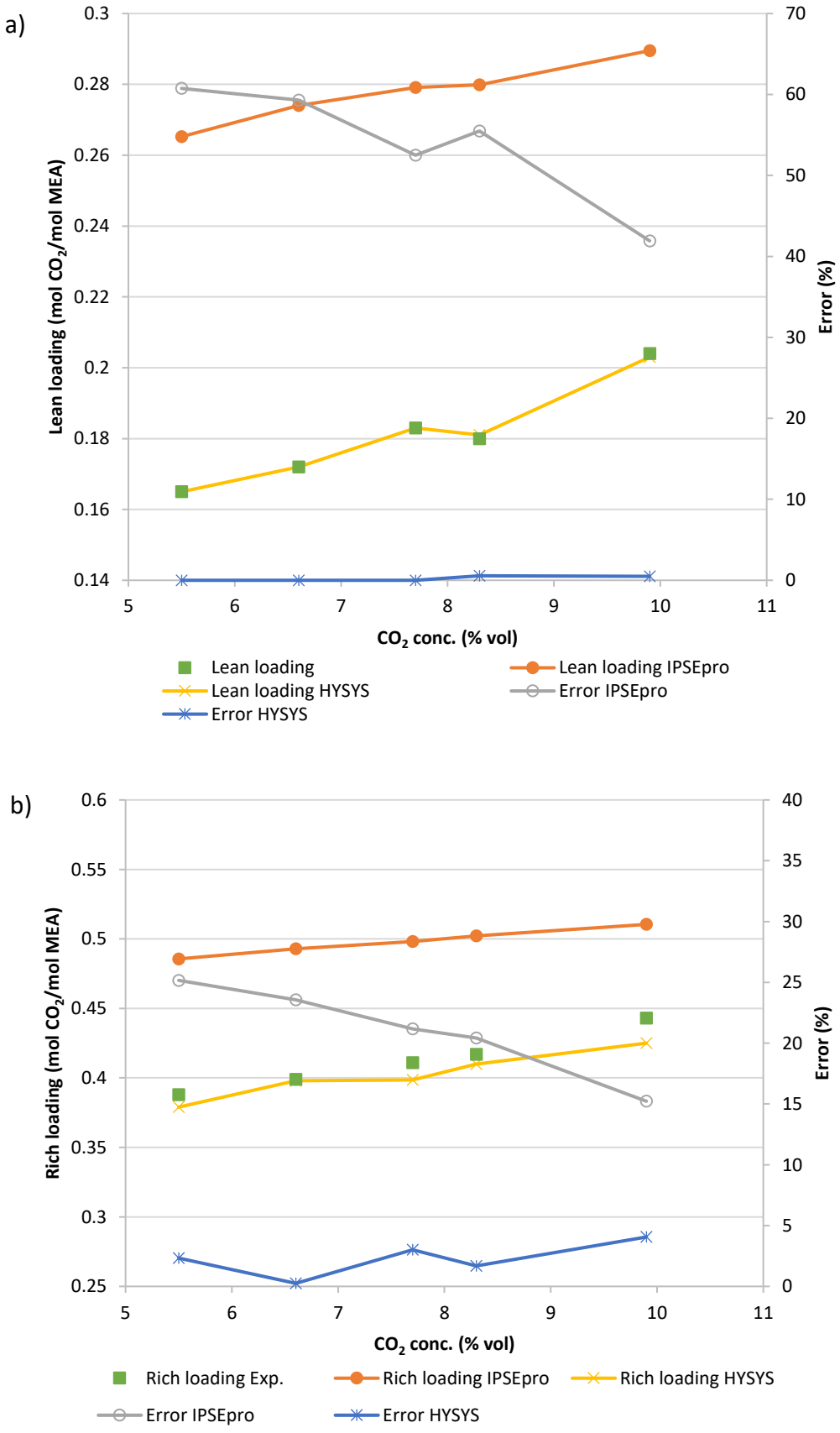

Figure 7: Variations of a) lean and b) rich CO_2 loading at various CO_2 concentration in the flue gas

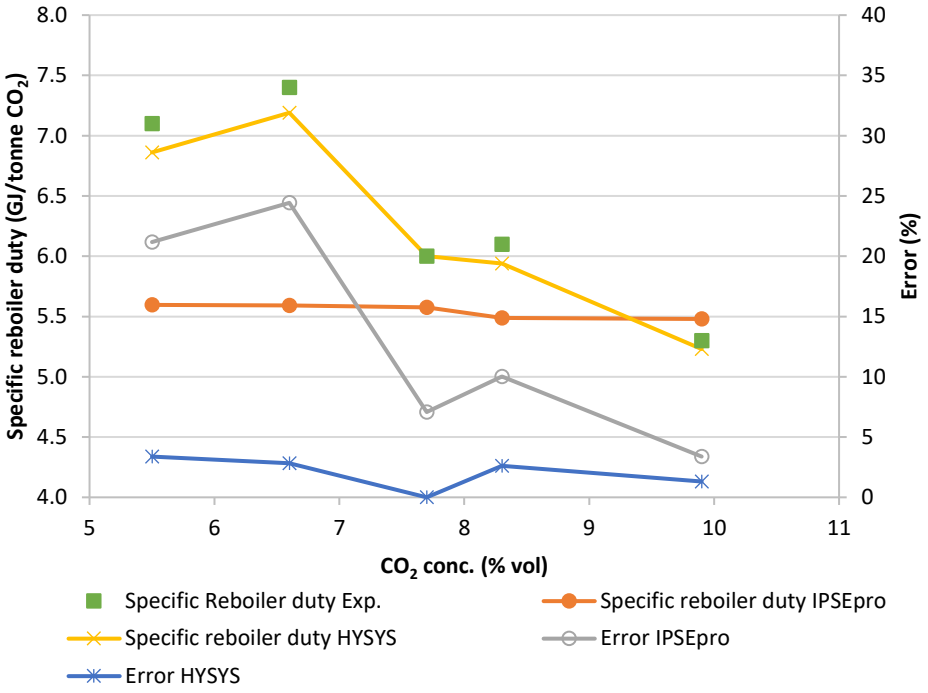

Figure 8: Specific reboiler duty at various CO_2 concentration in the flue gas

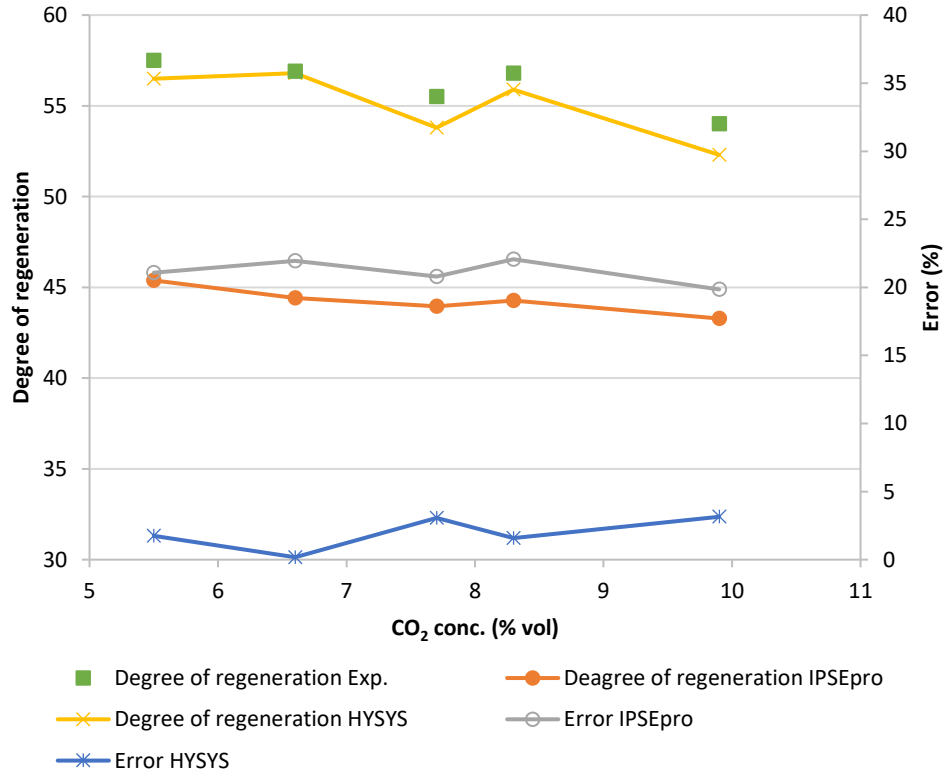

Figure 9: Degree of regeneration at various CO_2 concentration in the flue gas

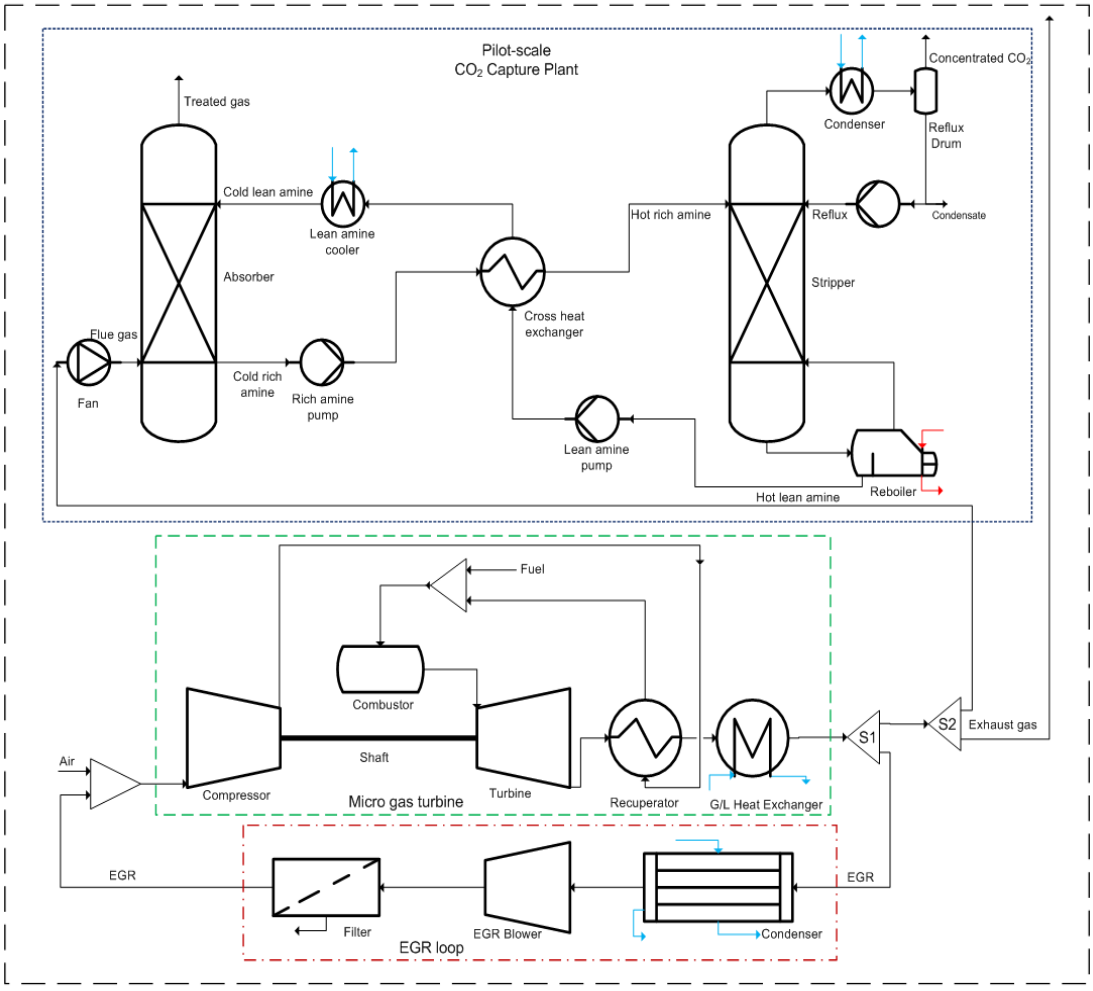

Figure 10: Schematic diagram of the integrated system of the MGT with EGR coupled to the pilot-scale CO_2 capture plant where the green dashed rectangle shows the MGT; the red dashed and dotted rectangle illustrates the EGR loop; and the blue dotted rectangle shows the pilot-scale CO_2 capture plant.

Table 1: Parameters monitored by LabView for the gas turbine at a frequency of 1 Hz.

Thermocouples		
TC1	system air inlet temperature	°C
TC2	compressed air temperature (compressor outlet)	°C
TC4	flue gas diffusion zone temperature	°C
TC5	flue gas outlet temperature	°C
TC6	cold water temperature (heat exchanger inlet)	°C
TC7	hot water temperature (heat exchanger outlet)	°C
TC8	ventilation air outlet temperature	°C
Pressure transducers		
PT1	system air inlet pressure	bar g
PT2	compressed air pressure (compressor outlet)	bar g
PT4	flue gas diffusion zone pressure	bar g
PT5	flue gas outlet pressure	bar g
PT6	ventilation air outlet pressure	bar g
Flowrate measurements		
FR1	system air inlet flowrate (total air in) – measured	kg/min
FR3	ventilation air outlet flowrate – measured	kg/min
FR4	flue gas outlet flowrate – calculated	kg/min

Table 2: Natural gas and air compositions

Component	**Mole Fraction**
Natural Gas Composition*	
CH_4	0.906
C_2H_6	0.051
C_3H_8	0.013
n-C_4H_{10}	0.002
i-C_4H_{10}	0.002
N_2	0.011
CO_2	0.014
Air Composition	
N_2	0.773
O_2	0.207
Ar	0.009
CO_2	0.0003
H_2O	0.001

*Natural gas composition obtained from National Grid

Table 3: Assumptions for the reference MGT model

Parameter	**Unit**	**Value**
Ambient temperature	°C	15
Ambient pressure	bar	1.013
Relative humidity	%	60
Net electrical power output	kW	100
Turbine outlet pressure	bar	1.06
Turbine outlet temperature	°C	650
HEX water inlet temperature	°C	50
HEX outlet water temperature	°C	70
Recuperator effectiveness	%	91
HEX water pressure	bar	1.013
HEX gas outlet temperature	°C	55

Table 4: Summary of experimental results – gas turbine parameters and emissions – for different power outputs/setpoints used to validate the gas turbine models.

Variable	**50 kW_e (Baseload)**	**60 kW_e**	**70 kW_e**	**80 kW_e (Maximum)**
Fuel consumption (m^3/hr)	22.9	26.3	30.0	35.7
System flowrates				
FR1 (kg/min)	92	93	96	99
FR3 (kg/min)	61	61	61	59
FR4 (kg/min)	30	32	35	41
PGas (mbar)	6835	5973	5906	5764
Main – fuel valve opening (%)	44.48	57.14	63.80	75.7
Pilot – fuel valve opening (%)	15.87	20.31	20.90	22.18
Flue gas concentrations				
O_2 (vol%)	18.50	18.40	18.30	18.17
CO_2 (vol%)	1.40	1.51	1.59	1.66
CO (ppm)	22.4	2.2	1.8	0.0
NO (ppm)	11.62	12.57	12.05	8.68
NO_2 (ppm)	1.29	1.30	0.21	0.00
Total NOx (ppm)	12.91	13.87	12.25	10.16
CO_2 exhaust flowrate (kg/hr)	49.44	57.51	63.09	72.32
CO_2 intensity (g/kWh)	988.6	945.5	905.1	905.6

Table 5: T100 micro-turbine performance data at ISO condition.

Parameter	**Manufacturer Reference Data Series 1 [48]**	**Simulated (Hysys)**	**Simulated (IPSEpro)**
Electrical power output (kW_e)	100	100	100
LHV of natural gas (MJ/kg)		50.3	47.22
Thermal output (kW_{th})	165	165	159
Electrical efficiency (%)	30	30.2	31.1
Pressure ratio	4.50	4.54	4.41
Rotational speed (rpm)	70000	70000	69727
Turbine inlet temperature (ºC)	950	943	947
Turbine outlet temperature (ºC)	650	650	650
Fuel consumption (kW)	333	331	321
Flue gas flowrate (kg/s)*	0.8	0.76	0.77

* The fuel flowrate depends on the gas composition – this is specified for a fuel with a lower heating value (LHV) of 39 MJ/m_n^3

Table 6: Capture plant data used for model verification [41]

Case		**1**	**2**	**3**	**4**	**5**
CO_2 in flue gas (after CO_2 injection)	Vol (%)	5.5	6.6	7.7	8.3	9.9
Solvent flow	kg/h	400	488	567	604	721
CO_2 injection	kg/h	17	21	24.5	27	31.5
Flue gas flow to capture plant	Nm^3/h	210	210	210	210	210
Flue gas flow to capture plant	kg/h	257.8	260	261.5	262.4	264.7
Flue gas Temperature	°C	40	40	40	40	40
Lean solvent temperature	°C	40	40	40	40	40
PHW flow	m^3/h	7.43	7.43	7.43	7.43	7.43
PHW T_{Rin}	°C	120.6	120.4	120.8	120.5	120.5
PHW T_{Rout}	°C	115.8	114.5	115.3	114.5	114.7
Cold approach temperature T_{AC}[1]	°C	19.0	18.4	19	18.5	19.8
Hot approach temperature T_{AH}[2]	°C	19.7	19.0	20.0	19.8	19.2
Rich solvent concentration	wt.%	30.8	27.8	30.6	27.5	29.1
Lean solvent concentration	wt.%	31.9	29.9	31.7	29.8	30.5
Rich loading	molCO_2/molMEA	0.388	0.399	0.411	0.417	0.443
Lean loading	molCO_2/molMEA	0.165	0.172	0.183	0.18	0.204
Degree of regeneration	(%)	57.5	56.9	55.5	56.8	54.0
Mass flow of flue gas (after CO_2 injection	kg/h	242.1	245.8	246.4	247.9	248.4
Liquid to gas ratio	kg/kg	1.7	2.0	2.3	2.4	2.9
Solvent to CO_2 ratio	kg/kg	19.9	20.6	21.1	20.7	21.7
Specific reboiler duty	GJ/t CO_2	7.1	7.4	6.0	6.1	5.3
Stripper bottom temperature	°C	110.4	108.8	109.7	108.8	108.8
Wash column circulating liquid	°C	46.4	48.5	50.7	51.0	52.7
Wash column exit gas	°C	42.6	44.3	45.5	46.7	48.9
Absorber exit gas	°C	40.6	41.4	45.5	43.5	45.0
Flue gas temperature before fan	°C	32.5	29.0	32.8	29.6	29.2

[1]T_{AC} = Cold approach temperature
[2]T_{AH} = Hot approach temperature

Table 7: Micro gas turbine and pilot-scale amine-based CO_2 capture plant performance data with and without EGR.

Parameter	Simulated (Hysys)		Simulated (IPSEpro)	
EGR (%)	0	55	0	55
MGT				
Electrical power output (kW_e)	80	80	80	80
Electrical efficiency (%)	28.1	27.6	30.3	29.4
Pressure ratio	4.00	4.08	3.90	3.91
Rotational speed (rpm)	66800	66800	66132	66224
Turbine inlet temperature (°C)	896	897	913	911
Turbine outlet temperature (°C)	645	645	645	645
Fuel consumption (kW)	285	290	263.5	264
Flue gas flowrate (kg/s)[1]	0.70	0.69	0.69	0.69
Specific CO_2 emissions without CO_2 in air (g/kWh) [2]	690.6	692.5	670	671.3
Flue gas composition (mol %)				
O_2	17.71	14.68	17.74	14.67
CO_2	1.46	3.20	1.43	3.15
Ar	0.91	0.92	0.86	0.87
N_2	76.27	77.55	76.3	77.27
H_2O	3.65	3.64	3.65	4.02
O_2 concentration at the combustor inlet (mol %)	20.74	17.65	20.74	17.63
Exhaust gas flow rate (kg/s)	0.70	0.31	0.69	0.31
CO_2 capture plant				
Gas flowrate at absorber inlet (kg/s)	0.11	0.11	0.11	0.11
Lean amine flowrate (kg/s)	0.11	0.13	0.10	0.13
L/G ratio	1.0	1.2	0.94	1.2
Absorber inlet gas temperature (°C)	40	40	40	40
Absorber inlet liquid temperature (°C)	40	40	40	40
Lean amine strength (wt. %)	30	30	30	30
Lean amine loading (mol CO_2/ mol MEA)	0.2	0.2	0.397	0.317
Rich amine loading (mol CO_2/ mol MEA)	0.30	0.37	0.504	0.496
CO_2 capture rate (%)	90	90	90	90
Specific reboiler duty (GJ/kg CO_2)	10.7	6.0	10.16	6.53
Acid gas pick-up (mol/mol)	0.10	0.17	0.11	0.18

[1]The flue gas flowrate is before EGR splitter.

[2]The specific CO_2 emissions are reported without carbon capture and after the EGR splitter (after S1 in Figure 10) without accounting for CO_2 coming from air.